

Nonequilibrium Steady States and Fano-Kondo Resonances in an AB Ring with a Quantum Dot

JUNKO TAKAHASHI*, SHUICHI TASAKI

*Department of Applied Physics, School of Science and Engineering,
Waseda University, Tokyo 169-8555*

Electron transport through a strongly correlated quantum dot (QD) embedded in an Aharonov-Bohm (AB) ring is investigated with the aid of the finite- U slave-boson mean-field (SBMF) approach extended to nonequilibrium regime. A nonequilibrium steady state (NESS) of the mean-field Hamiltonian is constructed with the aid of the C^* -algebraic approach for studying infinitely extended systems. In the linear response regime, the Fano-Kondo resonances and AB oscillations of the conductance obtained from the SBFM approach are in good agreement with those from the numerical renormalization group technique (NRG) by Hofstetter *et al.* by using twice larger Coulomb interaction. At zero temperature and finite bias voltage, the resonance peaks of the differential conductance tend to split into two. At low bias voltage, the split of the asymmetric resonance can be observed as an increase of the conductance plateau. We also found that the differential conductance has zero-bias maximum or minimum depending on the background transmission via direct tunneling between the electrodes.

KEYWORDS: Fano-Kondo resonance, nonequilibrium steady states, AB oscillation, quantum dot, AB ring, finite- U slave-boson mean-field approach, C^* -algebra

*E-mail address: junchi@ruri.waseda.jp

1. Introduction

Coherent transports of electrons through a quantum dot (QD) embedded in an Aharonov-Bohm (AB) ring have been widely studied in recent years. For such systems, interference between the localized states in the QD and the continuous states in the direct scattering channel causes asymmetric resonance peaks in the conductance,^{1,2} the so-called Fano resonances.³ On the other hand, strong Coulomb interaction induces the Kondo effect, i.e., the formation of a singlet bound state among localized and conduction electrons. In case of transport through single QD, it is seen as a plateau in the resonance tunneling peak, where the conductance reaches the unitary limit value ($2e^2/h$). Thus, when the Coulomb interaction is strong enough, an interplay between the Fano and Kondo effects is expected in the AB ring with a QD.

In the linear response regime, the interplay was theoretically studied by Hofstetter *et al.*, employing the numerical renormalization group (NRG) technique,⁴ and they predicted suppression of the Kondo plateau by the Fano resonance (the Fano-Kondo resonance). Such a behavior has been observed by recent experiments.^{5,6} They also studied the AB oscillations in the plateau regime⁴ and showed that the phase of the AB-oscillation is almost fixed at $\pi/2$ ⁷ and its frequency is almost doubled, both relative to the AB-oscillation at higher gate voltage.

Outside the linear response regime, the conductance maximum at zero bias voltage^{8,9} characterizes the Kondo effect in the transport through a single QD. The conductance drop at finite bias voltage is considered to be due to inelastic scattering involving electrons with energy between the chemical potentials of the two electrodes in case of infinite Coulomb repulsion. An AB ring with a QD is predicted to have a conductance minimum or maximum at zero bias voltage depending on the magnetic field.¹⁰ In spite of these researches, we think that the nonequilibrium properties of an AB ring with a QD particularly in case of large but finite Coulomb interaction are not fully understood partly because of the lack of complete characterization of nonequilibrium ensembles.

On the other hand, the method of C*-algebra has been widely applied to rigorous investigations of nonequilibrium steady states (NESSs) of infinitely extended quantum systems.^{11–21} The method was originally developed to deal with equilibrium statistical mechanics^{22–24} and, then, found to be useful also for studying nonequilibrium properties.^{11–21} Particularly, Fröhlich, Merkli and Ueltschi²¹ have shown the existence of NESS and its characterization for junction systems, which consist of several free-fermionic reservoirs mutually interacting via bounded interactions. Their results cover the AB ring with a QD in case that the electrodes are free fermion systems, but explicit characterizations of NESS are not given.

In this paper, we investigate the transports in an AB ring with a single-level QD, employing the finite- U slave-boson mean-field (SBMF) approach of Kotliar and Ruckenstein²⁵ extended to nonequilibrium steady states. The NESS with respect to the mean-field Hamilto-

nian is constructed based on the C^* -algebraic approach as in the noninteracting case.^{26,27} The infinite- U ^{28–36} and finite- U ^{37–45} SBMF approaches in combination with the Keldysh Green function method are successfully applied to the study of strongly correlated systems. In particular, the main features of the Kondo effect in the transport through a single QD such as the conductance plateau and the zero-bias maximum have been well described by the finite- U SBMF approach.^{38,42} In contrast to these works, we focus on the finite- U case and treat the mean-field NESS in terms of the C^* -algebraic approach, which leads to a global characterization of NESSs and, we believe, has an advantage compared to the Keldysh method in this respect.

The rest of this paper is arranged as follows. In Sec.2, after describing the model of the AB ring with a QD and reviewing the slave-boson description of Kotliar and Ruckenstein, the nonequilibrium SBMF approximation is explained. Relations among mean-fields and Lagrange multipliers are derived from the equations of motion of the auxiliary bosons within Dirac's formulation of constrained dynamics in contrast to the original SBMF approach,²⁵ which is based on the saddle-point approximation of the path integral representation of the free energy. The self-consistent equations are closed by evaluating the averages of certain fermionic variables with respect to a NESS for the mean-field Hamiltonian, which is constructed with the aid of the C^* -algebraic approach. Section 3 is devoted to the summary of the self-consistent equations and the derivation of the average current. Within this approximation, the Coulomb interaction is shown to result in the renormalization of the dot energy and the reduction of the dot level-width. In Sec.4, we study the conductance in the linear response regime and show that (i) the Fano-Kondo resonances and AB oscillations obtained from the SBMF approach are in good agreement with the results from the NRG technique by employing twice large Coulomb energy.⁴ In addition, the SBMF approach is shown to give a simple view to the underlying physical processes. In Sec.5, we study the differential conductance at fixed average number of dot electrons. We have found that (ii) the Fano-Kondo resonances are deformed by the bias voltage so that the resonance peaks have the tendency to split into two peaks and that (iii) the differential conductance may have zero-bias maximum or minimum depending on the transmission via the direct tunneling between the electrodes. The former is due to the narrowing of the dot level-width by the Kondo effect and, at low bias voltage, can be observed as an increase of the conductance plateau, which is consistent with the recent observation by Katsumoto *et. al.* for the T-shaped QD systems.⁵ Section 6 is devoted to concluding remarks. In Appendix, we explain the details of the construction of asymptotic field operators necessary for the construction of NESS.

2. Nonequilibrium Slave-Boson Mean-Field Approach

2.1 Model and slave-boson approach

Our system is described by the Anderson single impurity Hamiltonian⁴⁶ with the direct channel between left and right electrodes:

$$H = H_L + H_R + H_D + H_T + H_{LR}. \quad (1)$$

The first and second term are Hamiltonians of the two-dimensional electrodes

$$H_r = \sum_{\sigma} \int dk \omega_{kr} a_{k\sigma r}^{\dagger} a_{k\sigma r} \quad (r = L \text{ or } R) \quad (2)$$

where ω_{kr} is the single-electron energy: $\omega_{kL} = \omega_{kR} - eV = \hbar^2 k^2 / (2m) - eV/2$ with V the bias voltage and m the effective mass, and $a_{k\sigma r}^{\dagger}$ ($a_{k\sigma r}$) is the creation (annihilation) operator of the electrode electron with wave number k and spin σ . The third term H_D describes the single-level dot with the Coulomb interaction U :

$$H_D = \sum_{\sigma} \epsilon_{\sigma} c_{\sigma}^{\dagger} c_{\sigma} + U n_{\uparrow} n_{\downarrow} \quad (3)$$

where c_{σ}^{\dagger} (c_{σ}) is the creation (annihilation) operator of electrons in the dot, $n_{\sigma} = c_{\sigma}^{\dagger} c_{\sigma}$ the number operator and ϵ_{σ} the single-level energy. The tunneling between the dot and electrodes is given by

$$H_T = \sum_{\sigma} \int dk [u_{kL} a_{k\sigma L}^{\dagger} c_{\sigma} + u_{kR} a_{k\sigma R}^{\dagger} c_{\sigma} + (\text{H.c.})] \quad (4)$$

and the transmission through the direct channel by

$$H_{LR} = \sum_{\sigma} \iint dk dq [W u_{kL} u_{qR} e^{i\varphi} a_{k\sigma L}^{\dagger} a_{q\sigma R} + (\text{H.c.})], \quad (5)$$

where the tunneling matrix elements u_{kL} , u_{kR} and $W u_{kL} u_{qR}$ (hence W) are taken to be real. Because the resonance shapes do not strongly depend on the functional form of the tunneling matrix elements, one can assume that the interaction Hamiltonian H_{LR} is separable as above without loss of generality. The AB phase φ is related to the magnetic flux Φ penetrating the ring via $\varphi = e\Phi/(\hbar c)$ with c the velocity of light.

In order to examine the transport through the strongly correlated QD, we employ the finite- U slave-boson mean-field (SBMF) approach proposed by Kotliar and Ruckenstein.²⁵ In order to describe the doubly occupied state as a bosonic single particle excitation, they have introduced four auxiliary bosonic fields \hat{e} , \hat{p}_{σ} ($\sigma = \uparrow, \downarrow$) and \hat{d} , respectively, labeling the empty, singly occupied and doubly occupied states, and a fermionic field f_{σ} , describing the fermionic feature of the QD electrons. The expression of the Hamiltonian (1) in terms of the new variables is obtained by replacing the original QD electron operators as follows:

$$\begin{aligned} c_{\sigma}^{\dagger} c_{\sigma} &\rightarrow f_{\sigma}^{\dagger} f_{\sigma} \\ n_{\uparrow} n_{\downarrow} &\rightarrow \hat{d}^{\dagger} \hat{d} \\ c_{\sigma} &\rightarrow \hat{z}_{\sigma} f_{\sigma} \end{aligned}$$

where \hat{z}_σ is a bosonic variable defined by

$$\hat{z}_\sigma = (1 - \hat{d}^\dagger \hat{d} - \hat{p}_\sigma^\dagger \hat{p}_\sigma)^{-1/2} (\hat{e}^\dagger \hat{p}_\sigma + \hat{p}_\sigma^\dagger \hat{d}) (1 - \hat{e}^\dagger \hat{e} - \hat{p}_\sigma^\dagger \hat{p}_\sigma)^{-1/2}. \quad (6)$$

The additional degrees of freedom simplify the Coulomb interaction $Un_\uparrow n_\downarrow$ as $U\hat{d}^\dagger \hat{d}$, but, at the same time, introduce vectors not describing physical states. Then, physical vectors $|\Phi_{ph}\rangle$ are picked up by a set of constraints

$$\begin{aligned} \hat{\phi}_{1\sigma} |\Phi_{ph}\rangle &\equiv (\hat{p}_\sigma^\dagger \hat{p}_\sigma + \hat{d}^\dagger \hat{d} - f_\sigma^\dagger f_\sigma) |\Phi_{ph}\rangle = 0 \\ \hat{\phi}_2 |\Phi_{ph}\rangle &\equiv (\hat{e}^\dagger \hat{e} + \hat{d}^\dagger \hat{d} + \sum_\sigma \hat{p}_\sigma^\dagger \hat{p}_\sigma - 1) |\Phi_{ph}\rangle = 0 \end{aligned} \quad (7)$$

As easily seen, the subspace of the enlarged Hilbert space defined by (7) is equivalent to the original Hilbert space. Note that, since $\hat{\phi}_{1\sigma}$, $\hat{\phi}_2$ and H commute with each other, no further constraints are necessary.

As discussed in detail by Dirac,⁴⁷⁻⁴⁹ corresponding to the constraints $\hat{\phi}_{1\sigma} |\Phi_{ph}\rangle = 0$ and $\hat{\phi}_2 |\Phi_{ph}\rangle = 0$, q -number Lagrange multipliers $\hat{\lambda}_\sigma^{(1)}$ and $\hat{\lambda}^{(2)}$ should be introduced to the Heisenberg equation of motion and, with respect to the effective Hamiltonian $\tilde{H} \equiv H + \sum_\sigma \hat{\lambda}_\sigma^{(1)} \hat{\phi}_{1\sigma} + \hat{\lambda}^{(2)} \hat{\phi}_2$, any dynamical variable A satisfies the standard equation of motion as a state equation

$$\frac{dA}{dt} |\Phi_{ph}\rangle = \frac{i}{\hbar} [\tilde{H}, A] |\Phi_{ph}\rangle \quad (8)$$

where $|\Phi_{ph}\rangle$ is an arbitrary physical state and the explicit expression of \tilde{H} is

$$\begin{aligned} \tilde{H} &= H_L + H_R + H_{LR} + \sum_\sigma \int dk [\hat{z}_\sigma^\dagger (u_{kL} f_\sigma^\dagger a_{k\sigma L} + u_{kR} f_\sigma^\dagger a_{k\sigma R}) + (H.C.)] + U\hat{d}^\dagger \hat{d} \\ &+ \sum_\sigma \epsilon_\sigma f_\sigma^\dagger f_\sigma + \sum_\sigma \lambda_\sigma^{(1)} (\hat{p}_\sigma^\dagger \hat{p}_\sigma + \hat{d}^\dagger \hat{d} - f_\sigma^\dagger f_\sigma) + \lambda^{(2)} (\hat{e}^\dagger \hat{e} + \hat{d}^\dagger \hat{d} + \sum_\sigma \hat{p}_\sigma^\dagger \hat{p}_\sigma - 1). \end{aligned} \quad (9)$$

Note that, under the constraints (7), the equation of motion (8) is equivalent to the Heisenberg equation of motion with respect to the original Hamiltonian (1).

2.2 Nonequilibrium mean field approximation

The key idea of the SBMF approximation is to replace all the slave-boson operators and the Lagrange multipliers by their average values, which will be denoted as $e, p_\sigma, d, \lambda_\sigma^{(1)}$ and $\lambda^{(2)}$, and to impose, instead of (7), weaker constraints among averages:

$$|e|^2 + |d|^2 + \sum_\sigma |p_\sigma|^2 = 1 \quad (10)$$

$$\langle f_\sigma^\dagger f_\sigma \rangle_{ss} = |d|^2 + |p_\sigma|^2, \quad (11)$$

where $\langle f_\sigma^\dagger f_\sigma \rangle_{ss}$ stands for an average of $f_\sigma^\dagger f_\sigma$. This approximation can be extended to nonequilibrium steady states (NESSs) by regarding $e, p_\sigma, d, \lambda_\sigma^{(1)}, \lambda^{(2)}$ and $\langle f_\sigma^\dagger f_\sigma \rangle_{ss}$ as the NESS averages with respect to the mean field effective Hamiltonian:

$$H_{eff} = H_F + U|d|^2 + \sum_\sigma \lambda_\sigma^{(1)} (|p_\sigma|^2 + |d|^2) + \lambda^{(2)} (|e|^2 + |d|^2 + \sum_\sigma |p_\sigma|^2 - 1) \quad (12)$$

where H_F is the fermionic part:

$$H_F = H_L + H_R + H_{LR} + \sum_{\sigma} \int dk [z_{\sigma}^* (u_{kL} f_{\sigma}^{\dagger} a_{k\sigma L} + u_{kR} f_{\sigma}^{\dagger} a_{k\sigma R}) + (H.C.)] + \sum_{\sigma} \bar{\epsilon}_{\sigma} f_{\sigma}^{\dagger} f_{\sigma}, \quad (13)$$

$\bar{\epsilon}_{\sigma} = \epsilon_{\sigma} - \lambda_{\sigma}^{(1)}$ is the effective energy of the QD level and the mean value z_{σ} is obtained from (6) by replacing the bosonic operators to their averages. The characterization and properties of NESS with respect to H_{eff} will be discussed in the next subsection.

We have seven averages to be determined and the constraints provide three conditions. Hence, four more conditions are necessary. Originally, Kotliar and Ruckenstein²⁵ derived them by the saddle-point approximation for the equilibrium free energy, but this approach can not be applied to NESS. Here, we derive those conditions from the equations of motion of the slave boson fields. For example, \hat{d} obeys the equation of motion:

$$i\hbar \frac{d}{dt} \hat{d} = - \sum_{\sigma} \int dk \{ [\hat{z}_{\sigma}^{\dagger}, \hat{d}] (u_{kL} f_{\sigma}^{\dagger} a_{k\sigma L} + u_{kR} f_{\sigma}^{\dagger} a_{k\sigma R}) + [\hat{z}_{\sigma}, \hat{d}] (u_{kL} a_{k\sigma L}^{\dagger} f_{\sigma} + u_{kR} a_{k\sigma R}^{\dagger} f_{\sigma}) \} + (U + \sum_{\sigma} \lambda_{\sigma}^{(1)} + \lambda^{(2)}) \hat{d}. \quad (14)$$

By replacing the slave-boson operators and Lagrange multipliers to their mean values and by evaluating NESS averages of the fermionic operators, one gets

$$\sum_{\sigma} \left(\frac{\partial z_{\sigma}^*}{\partial d^*} M_{\sigma} + \frac{\partial z_{\sigma}}{\partial d^*} M_{\sigma}^* \right) + (U + \sum_{\sigma} \lambda_{\sigma}^{(1)} + \lambda^{(2)}) d = i\hbar \frac{d}{dt} d = 0 \quad (15)$$

where $M_{\sigma} = \int dk \langle u_{kL} f_{\sigma}^{\dagger} a_{k\sigma L} + u_{kR} f_{\sigma}^{\dagger} a_{k\sigma R} \rangle_{ss}$. Here, the average of $[\hat{z}_{\sigma}, \hat{d}]$ is evaluated as

$$\begin{aligned} [\hat{z}_{\sigma}, \hat{d}] &= [(1 - \hat{d}^{\dagger} \hat{d} - \hat{p}_{\sigma}^{\dagger} \hat{p}_{\sigma})^{-1/2}, \hat{d}] (\hat{e}^{\dagger} \hat{p}_{\sigma} + \hat{p}_{\sigma}^{\dagger} \hat{d}) (1 - \hat{e}^{\dagger} \hat{e} - \hat{p}_{\sigma}^{\dagger} \hat{p}_{\sigma})^{-1/2} \\ &= \sum_{n=1}^{\infty} \frac{(2n-1)!!}{(2n)!!} [(\hat{d}^{\dagger} \hat{d} + \hat{p}_{\sigma}^{\dagger} \hat{p}_{\sigma})^n, \hat{d}] (\hat{e}^{\dagger} \hat{p}_{\sigma} + \hat{p}_{\sigma}^{\dagger} \hat{d}) (1 - \hat{e}^{\dagger} \hat{e} - \hat{p}_{\sigma}^{\dagger} \hat{p}_{\sigma})^{-1/2} \\ &= - \sum_{n=1}^{\infty} \frac{(2n-1)!!}{(2n)!!} \sum_{l=0}^{n-1} (\hat{d}^{\dagger} \hat{d} + \hat{p}_{\sigma}^{\dagger} \hat{p}_{\sigma})^{n-1-l} \hat{d} (\hat{d}^{\dagger} \hat{d} + \hat{p}_{\sigma}^{\dagger} \hat{p}_{\sigma})^l (\hat{e}^{\dagger} \hat{p}_{\sigma} + \hat{p}_{\sigma}^{\dagger} \hat{d}) (1 - \hat{e}^{\dagger} \hat{e} - \hat{p}_{\sigma}^{\dagger} \hat{p}_{\sigma})^{-1/2} \\ &\rightarrow - \sum_{n=1}^{\infty} \frac{(2n-1)!!}{(2n)!!} n (|d|^2 + |p_{\sigma}|^2)^{n-1} d (e^* p_{\sigma} + p_{\sigma}^* d) (1 - |e|^2 - |p_{\sigma}|^2)^{-1/2} = - \frac{\partial z_{\sigma}}{\partial d^*} \end{aligned}$$

and that of $[\hat{z}_{\sigma}^{\dagger}, \hat{d}]$ as $-\frac{\partial z_{\sigma}^*}{\partial d^*}$. Similarly, from the equations of motion of \hat{e} and \hat{p}_{σ} , one has

$$\sum_{\sigma} \left(\frac{\partial z_{\sigma}^*}{\partial e^*} M_{\sigma} + \frac{\partial z_{\sigma}}{\partial e^*} M_{\sigma}^* \right) + \lambda^{(2)} e = 0 \quad (16)$$

$$\sum_{\tau} \left(\frac{\partial z_{\tau}^*}{\partial p_{\sigma}^*} M_{\tau} + \frac{\partial z_{\tau}}{\partial p_{\sigma}^*} M_{\tau}^* \right) + (\lambda_{\sigma}^{(1)} + \lambda^{(2)}) p_{\sigma} = 0 \quad (17)$$

When one neglects the Zeeman effect as in this article, a straightforward investigation shows that e, p_{σ}, d and z_{σ} can be taken as real positive and, then, M_{σ} is real. Therefore, by

setting $d = \sqrt{D}$, $p_\sigma = \sqrt{P_\sigma}$, $e = \sqrt{E}$, the constraints (10), (11) and the conditions (15), (16), (17) cast into self-consistent equations for D and $\lambda_\sigma^{(1)}$:

$$z_\sigma = \frac{\sqrt{EP_\sigma} + \sqrt{DP_\sigma}}{\sqrt{(1-D-P_\sigma)(1-E-P_\sigma)}} \quad (18)$$

$$\lambda_\sigma^{(1)} = 2 \sum_\tau \left(\frac{\partial z_\tau}{\partial E} - \frac{\partial z_\tau}{\partial P_\sigma} \right) M_\tau \quad (19)$$

$$2 \sum_\sigma \frac{dz_\sigma}{dD} M_\sigma + U = 0 \quad (20)$$

where $\frac{d}{dD} = \frac{\partial}{\partial D} + \frac{\partial}{\partial E} - \sum_\tau \frac{\partial}{\partial P_\tau}$ and one should set $P_\sigma = \langle f_\sigma^\dagger f_\sigma \rangle_{ss} - D$, $E = D + 1 - \sum_\sigma \langle f_\sigma^\dagger f_\sigma \rangle_{ss}$ after evaluating all the derivatives.

2.3 Nonequilibrium steady states for the mean field Hamiltonian

Now we turn to the averages of fermionic operators which are evaluated at a nonequilibrium steady state (NESS) with respect to the fermionic part H_F of the effective Hamiltonian. Since we are interested in transports through mesoscopic contacts, we consider a NESS such that, very far from the contact, each electrode recovers equilibrium with individual temperatures and chemical potentials. According to the C*-algebraic approaches,^{13,14,16-18,21} an average of an observable A with respect to such a NESS is can be evaluated as

$$\langle A \rangle_{ss} = \lim_{t \rightarrow +\infty} \langle e^{i\frac{H_F}{\hbar}t} A e^{-i\frac{H_F}{\hbar}t} \rangle_0 \quad (21)$$

where $\langle A \rangle_0 \equiv \text{Tr}(\rho_l A)$ is the average with respect to a local equilibrium state ρ_l :⁵⁰

$$\rho_l = \frac{1}{\Xi} e^{-\beta_L(H_L - \mu_L N_L)} e^{-\beta_R(H_R - \mu_R N_R)}. \quad (22)$$

In the above, Ξ is the normalization constant, β_r , μ_r and N_r ($r = L, R$) are, respectively, the inverse temperature, chemical potential and the total number of particles: $N_r \equiv \sum_\sigma \int dk a_{k\sigma r}^\dagger a_{k\sigma r}$ of each electrode.

The existence and characterization of the NESS averages can be heuristically explained in terms of the Møller operator: $\widehat{\Omega} = \lim_{t \rightarrow -\infty} e^{iH_F t/\hbar} e^{-iH_0 t/\hbar}$ where $H_0 = H_L + H_R$. Indeed, since the initial density matrix ρ_l commutes with H_0 , one has

$$\langle A \rangle_{ss} = \lim_{t \rightarrow +\infty} \langle e^{-iH_0 t/\hbar} e^{iH_F t/\hbar} A e^{-iH_F t/\hbar} e^{iH_0 t/\hbar} \rangle_0 = \lim_{t \rightarrow -\infty} \langle e^{iH_0 t/\hbar} e^{-iH_F t/\hbar} A e^{iH_F t/\hbar} e^{-iH_0 t/\hbar} \rangle_0.$$

This seems to suggest $\langle A \rangle_{ss} = \langle \widehat{\Omega}^\dagger A \widehat{\Omega} \rangle_0$, but, as in the derivation of the Gell-Mann Low relation,⁵¹ the change of normalization should be taken into account and one obtains

$$\langle A \rangle_{ss} = \frac{\langle \widehat{\Omega}^\dagger A \widehat{\Omega} \rangle_0}{\langle \widehat{\Omega}^\dagger \widehat{\Omega} \rangle_0}. \quad (23)$$

According to the rigorous approaches,^{13,14,16-18,21} the existence of $\langle A \rangle_{ss}$ for an arbitrary finite observable A requires the absence of bound states of H_F , which is assumed throughout this article. In this case, $\widehat{\Omega} \widehat{\Omega}^\dagger = \mathbf{1}$ and $\widehat{\Pi} \equiv \widehat{\Omega}^\dagger \widehat{\Omega}$ is a projection onto the ortho-complement of the states involving dot electrons, namely, one should have $\widehat{\Pi} = (1 - f_\uparrow^\dagger f_\uparrow)(1 - f_\downarrow^\dagger f_\downarrow)$.⁵²

Simple characterization of the NESS is given in terms of the asymptotic fields. According to the scattering theory,⁵³ the Møller operator $\widehat{\Omega}$ generates an ‘in’ field: $\beta_{k\sigma\lambda}^\dagger \equiv \lim_{t \rightarrow -\infty} e^{iH_F t/\hbar} e^{-iH_0 t/\hbar} a_{k\sigma\lambda}^\dagger e^{iH_0 t/\hbar} e^{-iH_F t/\hbar} = \widehat{\Omega} a_{k\sigma\lambda}^\dagger \widehat{\Omega}^\dagger$, which creates ‘in’ states from the vacuum and satisfies the same anti-commutation relations as $a_{k\sigma r}$. Indeed, one has e.g.,

$$[\beta_{k\sigma r}, \beta_{k'\sigma'r'}^\dagger]_+ = \widehat{\Omega} a_{k\sigma r} \widehat{\Omega}^\dagger \widehat{\Omega} a_{k'\sigma'r'}^\dagger \widehat{\Omega}^\dagger + \widehat{\Omega} a_{k'\sigma'r'}^\dagger \widehat{\Omega}^\dagger \widehat{\Omega} a_{k\sigma r} \widehat{\Omega}^\dagger = \widehat{\Omega} [a_{k\sigma r}, a_{k'\sigma'r'}^\dagger]_+ \widehat{\Omega}^\dagger \widehat{\Omega} \widehat{\Omega}^\dagger \\ = \delta(k - k') \delta_{\sigma\sigma'} \delta_{rr'} \widehat{\Omega} \widehat{\Omega}^\dagger \widehat{\Omega} \widehat{\Omega}^\dagger = \delta(k - k') \delta_{\sigma\sigma'} \delta_{rr'} .$$

Also the intertwining relation $H_F \widehat{\Omega} = \widehat{\Omega} H_0$ shows that they are normal modes of H_F : $[H_F, \beta_{k\sigma r}] = \widehat{\Omega} [H_0, a_{k\sigma r}] \widehat{\Omega}^\dagger = -\omega_{kr} \widehat{\Omega} a_{k\sigma r} \widehat{\Omega}^\dagger = -\omega_{kr} \beta_{k\sigma r}$. The NESS averages of a product of ‘in’ fields are then calculated as follows:

$$\langle \beta_{k_1\sigma_1 r_1}^\dagger \beta_{k_2\sigma_2 r_2}^\dagger \beta_{k_3\sigma_3 r_3} \beta_{k_4\sigma_4 r_4} \rangle_{ss} = \langle \widehat{\Omega}^\dagger \beta_{k_1\sigma_1 r_1}^\dagger \beta_{k_2\sigma_2 r_2}^\dagger \beta_{k_3\sigma_3 r_3} \beta_{k_4\sigma_4 r_4} \widehat{\Omega} \rangle_0 / \langle \widehat{\Pi} \rangle_0 \\ = \langle \widehat{\Omega}^\dagger \widehat{\Omega} a_{k_1\sigma_1 r_1}^\dagger \widehat{\Omega}^\dagger \widehat{\Omega} a_{k_2\sigma_2 r_2}^\dagger \widehat{\Omega}^\dagger \widehat{\Omega} a_{k_3\sigma_3 r_3} \widehat{\Omega}^\dagger \widehat{\Omega} a_{k_4\sigma_4 r_4} \widehat{\Omega}^\dagger \widehat{\Omega} \rangle_0 / \langle \widehat{\Pi} \rangle_0 \\ = \langle \widehat{\Pi} a_{k_1\sigma_1 r_1}^\dagger \widehat{\Pi} a_{k_2\sigma_2 r_2}^\dagger \widehat{\Pi} a_{k_3\sigma_3 r_3} \widehat{\Pi} a_{k_4\sigma_4 r_4} \widehat{\Pi} \rangle_0 / \langle \widehat{\Pi} \rangle_0 \\ = \langle a_{k_1\sigma_1 r_1}^\dagger a_{k_2\sigma_2 r_2}^\dagger a_{k_3\sigma_3 r_3} a_{k_4\sigma_4 r_4} \widehat{\Pi}^4 \rangle_0 / \langle \widehat{\Pi} \rangle_0 \\ = \langle a_{k_1\sigma_1 r_1}^\dagger a_{k_2\sigma_2 r_2}^\dagger a_{k_3\sigma_3 r_3} a_{k_4\sigma_4 r_4} \rangle_0 \langle \widehat{\Pi} \rangle_0 / \langle \widehat{\Pi} \rangle_0 = \langle a_{k_1\sigma_1 r_1}^\dagger a_{k_2\sigma_2 r_2}^\dagger a_{k_3\sigma_3 r_3} a_{k_4\sigma_4 r_4} \rangle_0 ,$$

where we have used $[a_{k\sigma r}, \widehat{\Pi}] = 0$, $\widehat{\Pi}^4 = \widehat{\Pi}$ and the fact that $a_{k\sigma r}$ and f_σ (hence $\widehat{\Pi}$) are independent in the initial state ρ_l . Repeating the same arguments and reminding that the initial state ρ_l satisfies Wick’s theorem for $a_{k\sigma r}$, one finds that the NESS satisfies Wick’s theorem for the ‘in’ fields $\beta_{k\sigma r}$ and, in particular, the two-point functions are given by

$$\langle \beta_{k\sigma r}^\dagger \beta_{k'\sigma'r'} \rangle_{ss} = F_r(\omega_{kr}) \delta(k - k') \delta_{\sigma\sigma'} \delta_{rr'} . \quad (24)$$

where $F_r(\epsilon) = 1/(e^{\beta_r(\epsilon - \mu_r)} + 1)$ stands for the Fermi distribution function of each electrode. Reminding that the ‘in’ states are free particle states at $t = -\infty$, eq.(24) simply implies that the particles originally coming from the left (right) electrode carries its initial statistical information such as the temperature and chemical potential.

In order to close the self-consistent equations, one task is left, namely the construction of the ‘in’ fields. As shown in Appendix, they are obtained from an operator equation $[H_F, \beta_{k\sigma r}] = -\omega_{kr} \beta_{k\sigma r}$ with the boundary condition: $a_{k\sigma r}(t) \exp(i\omega_{kr} t/\hbar) \rightarrow \beta_{k\sigma r}$ as $t \rightarrow -\infty$. The so-obtained relations can be inverted and the original operators are expressed in terms of the ‘in’ fields:

$$f_\sigma = \sum_{r=L,R} \int dk z_\sigma u_{kr} \frac{\chi_\sigma(\omega_{kr})^* \beta_{k\sigma r}}{\Lambda_\sigma(\omega_{kr})^*} \quad (25)$$

$$a_{k\sigma r} = \beta_{k\sigma r} + \int dk' \left(\frac{z_\sigma^2 u_{kr} u_{k'r} \beta_{k'\sigma r}}{\omega_{k'r} - \omega_{kr} + i0} \frac{\xi_\sigma(\omega_{k'r})^*}{\Lambda_\sigma(\omega_{k'r})^*} + \frac{z_\sigma^2 u_{kr} u_{k'\bar{r}} \beta_{k'\sigma \bar{r}}}{\omega_{k'\bar{r}} - \omega_{kr} + i0} \frac{\kappa_\sigma(\omega_{k'\bar{r}})^*}{\Lambda_\sigma(\omega_{k'\bar{r}})^*} \right) \quad (26)$$

where $r = L$ or R and we abbreviate $\bar{L} = R$, $\bar{R} = L$. The auxiliary functions are defined as

$$\chi_\sigma(x) = 1 + W e^{i\varphi_r} \Omega_{\sigma r}(x) / z_\sigma \\ \Lambda_\sigma(x) = \nu_\sigma(x) (x - \bar{\epsilon}_\sigma) - \sum_r \Omega_{\sigma r}(x) - 2W \cos \varphi \Omega_{\sigma L}(x) \Omega_{\sigma R}(x) / z_\sigma$$

$$\begin{aligned}
\nu_\sigma(x) &= 1 - W^2 \Omega_{\sigma L}(x) \Omega_{\sigma R}(x) / z_\sigma^2 \\
\xi_\sigma(x) &= 1 + \Omega_{\sigma r}(x) [W^2(x - \bar{\epsilon}_\sigma) / z_\sigma^2 + 2W \cos \varphi / z_\sigma] \\
\kappa_\sigma(x) &= 1 + W e^{i\varphi r} (x - \bar{\epsilon}_\sigma) / z_\sigma
\end{aligned}$$

where $\Omega_{\sigma r}(x) = \int dk'' \frac{u_{k''r}^2 z_\sigma^2}{x - \omega_{k''r} - i0}$ and φ_L (φ_R) stands for φ ($-\varphi$).

By combining (25), (26) with (24), one can calculate $\langle f_\sigma^\dagger f_\sigma \rangle_{ss}$ and M_σ in (10), (11), (15), (16) and (17) (or in (18), (19) and (20)). This completes the derivation of the self-consistent equations. We note that, for equilibrium states, the self-consistent equations derived here reduce to those obtained by Kotliar and Ruckenstein²⁵ via a saddle-point approximation.

3. Basic Equations

From now on, we assume that the wave-number dependence of the tunneling matrix elements is weak so that $u_{kr} \equiv u_r$ ($r = L, R$) is constant and that the electrode-dot coupling is symmetric: $2\pi u_L^2 \rho_L = 2\pi u_R^2 \rho_R \equiv \Gamma$, where $\rho_{L/R}$ is the density of states of the left/right electrode. Moreover, we neglect the Zeeman energy and limit our attention to the spin degenerate case. Then, the mean fields, the average electron number per spin at the dot as well as the original dot-level are independent of the spin quantum number: $z_\uparrow = z_\downarrow \equiv z$, $\bar{\lambda}_\uparrow^{(1)} = \bar{\lambda}_\downarrow^{(1)} \equiv \lambda$, $\langle f_\uparrow^\dagger f_\uparrow \rangle_{ss} = \langle f_\downarrow^\dagger f_\downarrow \rangle_{ss} \equiv n$, and $\epsilon_\uparrow = \epsilon_\downarrow \equiv \epsilon_0$. And, the self-consistent equations (18), (19) and (20) read as

$$z = \frac{\sqrt{(n-D)(1+D-2n)} + \sqrt{D(n-D)}}{\sqrt{n(1-n)}} \quad (27)$$

$$\lambda = \frac{M}{\sqrt{n(1-n)}} \left[2\sqrt{\frac{n-D}{1+D-2n}} - \sqrt{\frac{1+D-2n}{n-D}} - \sqrt{\frac{D}{n-D}} + \frac{z(1-2n)}{\sqrt{n(1-n)}} \right] \quad (28)$$

$$4 \frac{dz}{dD} M + U = 0 \quad (29)$$

where

$$n = \frac{\Gamma z^2}{2\pi} (1 + z^4 x) \int d\epsilon \frac{1}{|\Lambda(\epsilon)|^2} (F_L(\epsilon) + F_R(\epsilon)) + \frac{\Gamma z^4}{\pi} \sqrt{x} \sin \varphi \int d\epsilon \frac{1}{|\Lambda(\epsilon)|^2} (F_L(\epsilon) - F_R(\epsilon)) \quad (30)$$

$$\begin{aligned}
M = \frac{\Gamma z}{2\pi} (1 + z^2 x) \int d\epsilon \frac{(\epsilon - \epsilon_0 + \lambda)}{|\Lambda(\epsilon)|^2} (F_L(\epsilon) + F_R(\epsilon)) \\
+ \frac{\Gamma z^2}{\pi} \sqrt{x} \sin \varphi \int d\epsilon \frac{(\epsilon - \epsilon_0 + \lambda)}{|\Lambda(\epsilon)|^2} (F_L(\epsilon) - F_R(\epsilon)) \quad (31)
\end{aligned}$$

with $|\Lambda(\epsilon)|^2 = [(1+x)(\epsilon/\Gamma - (\epsilon_0 - \lambda)/\Gamma) + \sqrt{x} z^2 \cos \varphi]^2 + z^4$ and $x \equiv \pi^2 W^2 u_L^2 \rho_L u_R^2 \rho_R$ measures the strength of the transmission via the direct tunneling. The chemical potentials μ_r of the electrodes, appeared in the Fermi distribution functions $F_r(\epsilon) = 1/(e^{\beta r(\epsilon - \mu_r)} + 1)$ ($r = L, R$), are taken to be $\mu_L = \mu - eV/2$, $\mu_R = \mu + eV/2$, where μ is the average chemical potential. The probability D of the double occupation at the dot level and the Lagrange multiplier λ are obtained as solutions of these self-consistent equations.

Now we turn to the average current at the nonequilibrium steady state. The current operator from left to right electrodes is expressed by the time derivative of the number operator of the left electrode $N_L = \sum_{\sigma} \int dk a_{k\sigma L}^{\dagger} a_{k\sigma L}$:

$$\begin{aligned} \hat{j} &\equiv -e \frac{d}{dt} N_L = \frac{ie}{\hbar} [N_L, \tilde{H}] \\ &= \frac{ie}{\hbar} \sum_{\sigma} \left[\int dk u_{kL} \hat{z}_{\sigma} a_{k\sigma L}^{\dagger} f_{\sigma} + \iint dk dq W u_{kL} u_{qR} e^{i\varphi} a_{k\sigma L}^{\dagger} a_{q\sigma R} - (\text{H.C.}) \right]. \end{aligned} \quad (32)$$

Its NESS average is given by

$$\begin{aligned} \langle \hat{j} \rangle_{ss} &= \frac{ie}{\hbar} \sum_{\sigma} \left[\int dk u_{kL} z_{\sigma} \langle a_{k\sigma L}^{\dagger} f_{\sigma} \rangle_{ss} + \iint dk dq W u_{kL} u_{qR} e^{i\varphi} \langle a_{k\sigma L}^{\dagger} a_{q\sigma R} \rangle_{ss} - (\text{c.c.}) \right] \\ &= -\frac{2e}{\hbar} \int_{\mu_c}^{\infty} d\epsilon T(\epsilon) \{F_L(\epsilon) - F_R(\epsilon)\}. \end{aligned} \quad (33)$$

where the first term is evaluated as $\langle \hat{z}_{\sigma} a_{k\sigma L}^{\dagger} f_{\sigma} \rangle_{ss} = z_{\sigma} \langle a_{k\sigma L}^{\dagger} f_{\sigma} \rangle_{ss}$ and (24) is used. In this equation, $T(\epsilon)$ is the transmission probability:

$$T(\epsilon) = \frac{z^4}{|\Lambda(\epsilon)|^2} \left\{ \left[\frac{2\sqrt{x}}{z^2} \left(\frac{\epsilon}{\Gamma} - \frac{\epsilon_0 - \lambda}{\Gamma} \right) + \cos \varphi \right]^2 + \sin^2 \varphi \right\}. \quad (34)$$

It is interesting to rewrite the transmission probability in the Fano form:^{4,54,55}

$$T(\epsilon) = T_b \frac{|\tilde{E} + q|^2}{\tilde{E}^2 + 1} \quad (35)$$

where $\tilde{E} = (1+x)\{(\epsilon - \epsilon_0 + \lambda)/(z^2\Gamma) + [\sqrt{x}/(1+x)]\cos\varphi\}$ and $T_b = 4x/(1+x)^2$ is the background transmission probability.⁴ The Fano parameter $q = [(1-x)\cos\varphi + i(1+x)\sin\varphi]/2\sqrt{x}$ takes into account the interference effect and determines the peak shape of the conductance. The conductance shows the Breit-Wigner type resonance if $x = 0$ (the real part of q is ∞) and the anti-resonance if $x = 1$ (the real part of q is 0). Eq. (35) also indicates that the SBMF approach takes into account the effect of Coulomb interaction in two ways, namely as renormalization of the dot energy by λ : $\epsilon_0 \rightarrow \epsilon_0 - \lambda$, and as reduction of the electrode-dot interaction by a factor of z^2 : $\Gamma \rightarrow z^2\Gamma$. The energy renormalization is partly taken into account in a simpler Hartree approximation. The reduction of the electrode-dot interaction implies the increase of the lifetime of the dot level and is interpreted as the stabilization of the dot level due to strong correlation between the conduction and localized electrons, which might be identified with precursor of the formation of a singlet quasi-bound state between the two and, thus, with development of the Kondo correlation.

In the following sections, we investigate transport properties at zero temperature, $1/\beta_L = 1/\beta_R = 0$, in detail.

4. Transports in Linear Response Regime

In this section, we focus on the linear response regime where the conductance is given by

$$G = \frac{2e^2}{h} T(\mu)$$

and the mean fields D and λ are determined by (27), (28), (29), (30) and (31) with $V = 0$. Then, we compare the results with those by the numerical renormalization group (NRG) technique.⁴

4.1 Fano-Kondo resonances

Figure 1 shows the conductance as a function of the original dot level ϵ_0 for various values of the background transmission probability T_b where the phase difference due to the magnetic flux, the electrode-dot coupling and the Coulomb energy are taken, respectively, as $\varphi = 0$, $\Gamma/\mu = 0.02$ and $U/\mu = 0.6$ with μ the average chemical potential. When $T_b = 0.0$, the conductance reaches the unitary limit $G = 2e^2/h$ and the well-known Kondo plateau is formed. With increasing the background transmission probability (cf. the curves for $T_b = 0.1, T_b = 0.3$), the Kondo plateau is modified by the Fano resonance due to the direct channel transport. When $T_b = 0.6$, the conductance curve has an asymmetric form, typically observed in the Fano resonance, with a large plateau between the peak and dip. The plateau is generated by the strong Coulomb interaction. Indeed, as shown in Fig. 2, the plateau region is gradually formed by increasing the Coulomb interaction. When the transport through the direct channel is dominant (i.e., $T_b = 1.0$), the destructive interference causes the anti-resonance. Such a behavior is experimentally observed in the T-shaped QD system.^{5,56}

We would like to remark that all the curves in Fig.1 are in good agreement with those in Fig.2 of Ref.4, that is obtained by the NRG technique. The parameters of the two results are almost the same except the strength of the Coulomb interaction $U/\Gamma \simeq 30$, which is almost twice larger than that of Ref.4. This indicates that the essential features of the conductance such as the shapes or peak positions are well captured by the SBMF approach in spite of neglecting the fluctuations of the bosonic fields and Lagrange multipliers.

4.2 Conductance plateau

Figure 2 indicates that strong Coulomb interaction is responsible for the plateau formation in the conductance curve. The underlying physical mechanism becomes more transparent by studying the average number of electrons per spin occupying the dot: n , and the probability of simultaneously finding two electrons at the dot: D . The left side of the upper panel in Fig.3 shows the conductance at $T_b = 0.6$ and the right side shows the average occupation number n , and the double occupation probability D . When the dot level is far above the Fermi energy ($\epsilon_0/\mu \gtrsim 1.0$), no electrons are found in the QD. As the dot level lowers, the occupation number n increases and reaches $1/2$ at $\epsilon_0/\mu \simeq 0.9$. Within the interval $0.5 \lesssim \epsilon_0/\mu \lesssim 0.9$, one sees $n \simeq 1/2$ and $D \simeq 0$, which implies that the dot is singly occupied and the second electron can not enter into the dot owing to the strong Coulomb interaction. In this interval, the electronic state does not change and, as a result, the conductance shows the wide plateau. When the dot level lowers further, the second electron starts to flow into the dot as indicated by the increase of the double occupation probability D , and the conductance again starts to form a

peak.

It is interesting to see the associated behavior of the SBMF parameters. The lower panels in Fig.3 show the reduction factor z^2 of the dot level-width and the renormalized dot energy $\epsilon_0 - \lambda$. Outside the plateau region $0.5 \lesssim \epsilon_0/\mu \lesssim 0.9$, $z^2 \simeq 1$ and $\epsilon_0 - \lambda \propto \epsilon_0 + (\text{const.})$. Hence, the dot level-width and the renormalized dot energy are the same as their bare values and the behavior of the system is essentially equivalent to that of the noninteracting case. On the other hand, within the plateau region $0.5 \lesssim \epsilon_0/\mu \lesssim 0.9$, $\epsilon_0 - \lambda$ is almost constant and z^2 is very small. The former indicates that the Coulomb interaction modifies the effective dot energy seen by the reservoir electrons so that the dot level is kept to be singly occupied. The latter indicates that the dot level-width is drastically suppressed by the Coulomb repulsion. The formation of the plateau is mainly due to the renormalization of the dot energy. As will be discussed in the next section, the effects of the reduction of the dot level-width can be seen more clearly in nonequilibrium regime.

4.3 Phase dependence of conductance

Figure 4 illustrates the phase dependence of the Fano-Kondo resonance. As in the noninteracting case, with changing the AB phase from $\varphi = 0$ to $\varphi = \pi$, the destructive interference between the localized and continuous states turns into the constructive interference and vice versa. On the other hand, the plateau of the two curves are almost the same. At $\varphi = \pi/2$, the conductance has a symmetric resonance peak and reaches the unitary limit value as in the case of $T_b = 0.0$ and $\varphi = 0$ (cf. Fig.1).

We now turn to the relation of the AB oscillations with the Fano-Kondo plateau. It was shown that the phase of the AB oscillation at one side of the conductance peak is different by π from that at the other side.^{57,58} Also the strong Coulomb interaction is known to fix the maximum position of the conductance at $\varphi \simeq \pi/2$ in the middle of the Fano-Kondo plateau.⁷ Figure 5 shows the conductance as a function of the AB phase φ for various occupation numbers n of the dot level. Outside the plateau regime ($n = 0.2, 0.8$), the conductance shows a 2π -periodic AB oscillation and does not reach the unitary-limit value $2e^2/h$. In contrast, in the plateau regime ($n = 0.45, 0.5, 0.55$), the conductance reaches the unitary limit $2e^2/h$ near $\varphi = \pi/2$ and is similar to a π -periodic sinusoidal curve. In other words, in the plateau regime, the period of the AB oscillation is almost fixed to be π and the conductance takes its maximum near $\varphi = \pi/2$. This behavior is different from the noninteracting case where the AB oscillation gradually changes its character as the increase of n .²⁶ Note that these features of the AB oscillation in the interacting case are consistent with the experiments and theoretical predictions of the works mentioned above.⁴⁻⁷

5. Transports in Nonequilibrium Regime

It is often argued that SBMF approaches are not appropriate for studying the dynamical properties of strongly correlated systems since they can not deal with the effect of charge

fluctuations.^{31,38} We have shown that the finite- U SBMF approach describes well, at least qualitatively, the transports of the AB ring with a QD in the linear response regime as compared with the NRG approach.⁴ So we believe that the SBMF approach could catch the essential features of the steady-state transports at finite bias voltage V . In this section, we study the properties of the differential conductance at fixed occupation number n :

$$G_n = \left(\frac{\partial \langle \hat{J} \rangle}{\partial V} \right)_n,$$

where the subscript n means that the V -derivative is taken by keeping n constant. Instead of the differential conductance at fixed dot level ϵ_0 , here we consider G_n because of a technical difficulty in solving the self-consistent equations. But the difference is small enough for describing the essential features except the region of $|hG_n/(2e^2)| \ll 1$. For example, at $\varphi = 0$, $\Gamma/\mu = 0.02$, $U/\mu = 0.6$, $n = 0.43$ and $eV/\mu = 0.002$, the difference is estimated to be at most 1%.

Figure 6 shows the ϵ_0 -dependence of G_n at $eV/\mu = 0.002$ for various values of the background transmission T_b with $\varphi = 0$, $\Gamma/\mu = 0.02$ and $U/\mu = 0.6$. At $T_b = 0.0$, the conductance plateau is suppressed by the low bias voltage. When $T_b = 0.3$, the bias voltage induces a peak in the conductance plateau. Such a behavior is recently observed in the side-coupled QD,⁵ which is one of the systems exhibiting the Fano resonance. As the background transmission increases, the resonance peak of the differential conductance tends to split into two asymmetric peaks (cf. the case of $T_b = 0.6$).

This could be understood as follows. Recall that the similar splitting of the resonance peak has been observed in the noninteracting case at higher bias voltage. In this case, a conductance peak is formed once the dot energy passes the Fermi level of the electrodes. At high bias voltage, two electrodes have very different Fermi energies and the two peaks are observed. While, if the bias voltage is so low that the difference between the Fermi levels is less than the width of the dot level, the two peaks are degenerate and one observes only one peak. On the other hand, as mentioned after (35), the transmission probability in the interacting case has the similar form as in the noninteracting case except the renormalization of the dot energy and the reduction of the dot level-width. Therefore, if the bias voltage is large enough compared with the level-width, two peaks can be observed. In the plateau regime, the reduction factor z^2 is small (cf. Fig. 3) and there appear two peaks even at very low bias voltage. In other words, because of the reduction of the width, the system becomes more sensitive to the bias voltage and the splitting of the resonance peak is observed at low bias voltage.

The differential conductance G_n is shown as a function of the bias voltage in Fig.7, Fig.8 and Fig.9 for various occupation numbers, where the other parameters are set again as $\varphi = 0$, $\Gamma/\mu = 0.02$ and $U/\mu = 0.6$. When the background conduction is absent $T_b = 0.0$ (i.e., in case

of the transport through a single QD), the conductance has a sharp peak at zero bias voltage. These peaks correspond to those experimentally observed in refs.8, 9. With decreasing the occupation number (this corresponds to the increase of ϵ_0 from the center of the conductance plateau of Fig.1), the zero-bias maximum is reduced from the unitary limit value $2e^2/h$ and the width of the peak becomes broader (cf. the curves at $n = 0.48, 0.43, 0.40$). This behavior of the zero-bias maximum agrees with the calculations reported by Craco *et al.*⁵⁹ and by B. Dong *et al.*^{38,60} Note that G_n at $n = 0.48$ has very small negative value for larger $|V|$, which seems to be an artifact due to the use of G_n .

In contrast, when the direct tunneling is turned on, the conductance changes its behavior. At $T_b = 0.6$ (Fig.8), there appears a zero bias dip and, similarly to the zero bias peak at $T_b = 0.0$, the dip width becomes broader as n decreases. Moreover, at $T_b = 0.45$ (Fig.9), a peak gradually changes into a broad dip as the decrease of n . In case of infinite Coulomb repulsion $U \rightarrow +\infty$, Buřka *et al.*¹⁰ predicts the possibility of the zero bias dip depending on the magnetic flux piercing the AB ring. Here we have shown that the similar behavior is possible depending on the strength of the background transmission.

6. Conclusions

We have investigated the transports through the QD embedded in the AB ring in the linear response and finite bias regimes, employing the nonequilibrium finite- U SBMF approach. The mean fields are evaluated at a nonequilibrium steady state with respect to the mean field Hamiltonian which is constructed with the aid of the C*-algebraic approaches. The Coulomb interaction is found to be taken into account as the renormalization of the dot energy and the reduction of the dot level-width. In particular, the latter may be interpreted as a signature of the formation of the singlet bound state between the dot and conduction electrons. We have studied the Fano-Kondo resonances and AB oscillations at the linear response regime and obtained the results which, by using twice larger Coulomb energy, are in good agreement with those by the numerical renormalization group (NRG) technique. Furthermore, this method is applied to the case with finite bias voltage, and we found that the Fano-Kondo plateau is suppressed and deformed by small bias voltage and that, in addition to the zero-bias peak, the zero-bias dip can be observed in the differential conductance depending on the strength of the background transmission.

It is interesting to give a rough estimate of the Kondo temperature. If the SBMF parameters were weakly dependent on temperature, the linear-response conductance at $T_b = 0$ and $\epsilon_0 - \lambda = \mu$ reads as

$$\frac{h}{2e^2}G = \int_{-\infty}^{+\infty} dy \left\{ 1 + \left(\frac{Ty}{z^2\Gamma} \right)^2 \right\}^{-1} \frac{e^y}{(e^y + 1)^2} \simeq 1 - \frac{1}{3} \left(\frac{\pi T}{z^2\Gamma} \right)^2 + \frac{7}{15} \left(\frac{\pi T}{z^2\Gamma} \right)^4 + \dots,$$

for $T/(z^2\Gamma) \ll 1$. By comparing this with the low temperature expansion of the empirical

formula⁶¹

$$\frac{h}{2e^2}G = \left(\frac{(2^{1/s} - 1)T_k^2}{T^2 + (2^{1/s} - 1)T_k^2} \right)^s,$$

where T_k stands for the Kondo temperature, one obtains $s = 5/37$ and $T_k \simeq 2.64 \times z^2\Gamma$. In case of $\Gamma/\mu = 0.02$ and $U/\mu = 0.6$, $z^2 \simeq 0.066$ and $T_k \simeq 375\text{mK}$ for $\mu = 9.29$ meV. The value is consistent with Haldane's formula:⁶²

$$T_k = \frac{1}{2} \left(\frac{\Gamma U}{2} \right)^{1/2} \exp \left\{ \frac{\pi \epsilon_0 (U + \epsilon_0)}{\Gamma U} \right\}$$

which leads to $T_k \simeq 443\text{mK}$ at $n = 0.48$ as well as the experimental value of $T_k = 450 \sim 460\text{mK}$.⁸ It should be noted that, without the reduction of the dot level-width, one would have a ten times larger value for the Kondo temperature. Moreover, this analysis shows that the reduction factor z^2 of the dot level-width is essentially the Kondo temperature and, thus, the ϵ_0 -dependence of z^2 (cf. Fig.3) can be reinterpreted as ϵ_0 -dependence of the Kondo temperature, which is parabolic near the center of the plateau and is consistent with experiments.⁸ These observations seem to support our interpretation that the reduction of the dot level-width implies the formation of the Kondo singlet. However, to confirm this view, the finite temperature case should be investigated and will be discussed elsewhere.

Acknowledgment

The authors thank Professor M. Eto, Professor S. Katsumoto, Professor S. Pascazio and Professor T. Kato for fruitful discussions and valuable comments. One of them (JT) thanks Professor S. Katsumoto for private discussion for informing them of ref.5 prior to publication. JT also thanks Professor T. Kato for information of ref.6 and thanks Dr. H. Aikawa and Mr. M. Sato for discussing on their these. This work is partially supported by a Grant-in-Aid for Scientific Research of Priority Areas "Control of Molecules in Intense Laser Fields" (No. 14077219) and the 21st Century COE Program at Waseda University "Holistic Research and Education Center for Physics of Self-organization Systems" both from the Ministry of Education, Culture, Sports, Science and Technology of Japan, a Grant-in-Aid for Scientific Research (C) (No.17540365) from the Japan Society of the Promotion of Science and Waseda University Grant for Special Research Projects (2004A-161, research promotion 2005).

Appendix: Construction of ‘in’ fields

Here we derive the ‘in’ fields and show (25) and (26). Thanks to the bilinearity of H_F , the ‘in’ fields $\beta_{k\sigma r}$ can be written as

$$\beta_{k\sigma r} = a_{k\sigma r} + g_r^{(1)}(k)f_\sigma + \sum_{r'} \int dk' g_{r:r'}^{(2)}(k, k') a_{k'\sigma r'} . \quad (\text{A}\cdot 1)$$

Substituting this into $[H_F, \beta_{k\sigma r}] = -\omega_{kr}\beta_{k\sigma r}$, we obtain e.g.,

$$(\omega_{kL} - \omega_{k'L})g_{L:L}^{(2)}(k, k') = u_{k'L} \left(z_\sigma g_L^{(1)}(k) + W e^{-i\varphi} \int dk'' g_{L:R}^{(2)}(k, k'') u_{k''R} \right)$$

and the boundary condition: $a_{k\sigma r}(t) \exp(i\omega_{kr}t/\hbar) \rightarrow \beta_{k\sigma r}$ (as $t \rightarrow -\infty$) gives

$$g_{L:L}^{(2)}(k, k') = \frac{u_{k'L}}{\omega_{kL} - \omega_{k'L} - i0} \left(z_\sigma g_L^{(1)}(k) + W e^{-i\varphi} \int dk'' g_{L:R}^{(2)}(k, k'') u_{k''R} \right) .$$

In the same way, a set of linear equations among six functions $g_r^{(1)}(k)$, $g_{r:r'}^{(2)}(k, k')$ ($r, r' = L, R$) is derived and its solution leads to

$$\begin{aligned} \beta_{k\sigma r} = & a_{k\sigma r} + \frac{\chi_\sigma(\omega_{kr})}{\Lambda_\sigma(\omega_{kr})} u_{kr} z_\sigma f_\sigma \\ & + \int dk' \left(\frac{z_\sigma^2 u_{kr} u_{k'r}}{\omega_{kr} - \omega_{k'r} - i0} \frac{\xi_\sigma(\omega_{kr})}{\Lambda_\sigma(\omega_{kr})} a_{k'\sigma r} + \frac{z_\sigma^2 u_{kr} u_{k'\bar{r}}}{\omega_{kr} - \omega_{k'\bar{r}} - i0} \frac{\kappa_\sigma(\omega_{kr})}{\Lambda_\sigma(\omega_{kr})} a_{k'\sigma\bar{r}} \right), \quad (\text{A}\cdot 2) \end{aligned}$$

where the notations are the same as those of (25) and (26). On the other hand, because of the completeness of $\beta_{k\sigma r}$ which is guaranteed by the absence of the bound states for H_F , one has

$$f_\sigma = \sum_r \int dk [f_\sigma, \beta_{k\sigma r}^\dagger]_+ \beta_{k\sigma r} ,$$

which gives (25). Eq.(26) can be derived similarly.

References

- 1) K. Kobayashi, H. Aikawa, S. Katsumoto and Y. Iye: Phys. Rev. Lett. **88** (2002) 256806.
- 2) K. Kobayashi, H. Aikawa, S. Katsumoto and Y. Iye: Phys. Rev. B **68** (2003) 235304.
- 3) U. Fano: Phys. Rev. **124** (1961) 1866.
- 4) W. Hofstetter, J. König and H. Schoeller: Phys. Rev. Lett. **87** 156803 (2001).
- 5) S. Katsumoto, M. Sato, H. Aikawa and Y. Iye: to be published in Physica E.
- 6) H. Aikawa: Dr. Thesis, Faculty of Science, The University of Tokyo, 2004.
- 7) U. Gerland, J. V. Delft, T. A. Costi and Y. Oreg: Phys. Rev. Lett. **84** (2000) 3710.
- 8) W. G. van der Wiel, S. De Franceschi, T. Fujisawa, J. M. Elzerman, S. Tarucha and L. P. Kouwenhoven: Science **289** (2000) 2105.
- 9) S. M. Cronenwett, T. H. Oosterkamp and L. P. Kouwenhoven: Nature **281** (1998) 540.
- 10) B. R. Bulka and P. Stefański: Phys. Rev. Lett. **86** (2001) 5128.
- 11) I. Ojima, H. Hasegawa and M. Ichiyanagi: J. Stat. Phys. **50** (1988) 633
- 12) I. Ojima: J. Stat. Phys. **56** (1989) 203 in *Quantum Aspects of Optical Communications*, (LNP **378**, Springer, 1991).
- 13) D. Ruelle: J. Stat. Phys. **98** (2000) 57.
- 14) D. Ruelle: Comm. Math. Phys. **224** (2001) 3.
- 15) T.G. Ho and H. Araki: *Proc. Steklov Math. Institute* **228** (2000) 191.
- 16) V. Jakšić and C.-A. Pillet: Commun. Math. Phys. **217** (2001) 285.
- 17) V. Jakšić and C.-A. Pillet: Commun. Math. Phys. **226** (2002) 131.
- 18) V. Jakšić and C.-A. Pillet: J. Stat. Phys. **108** (2002) 269 and references therein.
- 19) S. Tasaki: Chaos, Solitons and Fractals, **12** 2657 (2001).
- 20) S. Tasaki, T. Matsui: in *Fundamental Aspects of Quantum Physics* eds. L. Accardi, S. Tasaki: World Scientific, Singapore, (2003) p.100 and references therein.
- 21) J. Fröhlich, M. Merkli, D. Ueltschi: *Ann. Henri Poincaré* **4** (2003) 897 (2003).
- 22) O. Bratteli and D.W. Robinson: *Operator Algebras and Quantum Statistical Mechanics* vol.1 (Springer, New York, 1987); vol.2, (Springer, New York, 1997).
- 23) D. Ruelle: *Statistical Mechanics: Rigorous Results*, (Benjamin, Reading, 1969)
- 24) Ya. G. Sinai: *The Theory of Phase Transitions: Rigorous Results*, (Pergamon, Oxford, 1982).
- 25) G. Kotliar and A. E. Ruckenstein: Phys. Rev. Lett. **57** (1986) 1362.
- 26) J. Takahashi and S. Tasaki: *Statistical Physics of Quantum Systems - novel orders and dynamics-*, J. Phys. Soc. Jpn. suppl. **74** (2005) pp.261-264.
- 27) J. Takahashi and S. Tasaki: to be published in Physica E.
- 28) T. Aono, M. Eto and K. Kawamura, J. Phys. Soc. Jpn. **67** (1998) 1860.
- 29) T. Aono and M. Eto: Phys. Rev. B **63** (2001) 125327.
- 30) T. Aono and M. Eto: Phys. Rev. B **64** (2001) 073307.
- 31) R. Aguado and D. C. Langreth, Phys. Rev. Lett. **85** (2000) 1946.
- 32) W. S. Quan and W. S. Jin: Chin. Phys. Lett. **20** (2003) No.9 1574.
- 33) B. Dong and X. L. Lei: J. Phys.: Condens. Matter **15** (2003) 8435.
- 34) K. Kang, S. Y. Cho, J. J. Kim and S. C. Shin: Phys. Rev. B **63** (2001) 113304.
- 35) B. H. Wu, J. C. Cao and K. H. Ahn: Phys. Rev. B **72** (2005) 165313.
- 36) P. Simon, O. E. Wohlmann and A. Aharony: cond-mat/0507309.

- 37) B. Dong and X. L. Lei: Phys. Rev. B **63** (2001) 235306.
- 38) B. Dong and X. L. Lei: J. Phys. Condens. Matter **13** (2001) 9245.
- 39) B. Dong and X. L. Lei: Phys. Rev. B **65** (2002) 241304(R).
- 40) B. Dong and X. L. Lei: Phys. Rev. B **66** (2002) 113310.
- 41) B. Dong and H. L. Cui: Semicond. Sci. Technol. **19** (2004) No.4 S14.
- 42) B. Dong, G. H. Ding, H. L. Cui and X. L. Lei: Europhys. Lett. **69** (3) (2005) 424.
- 43) J. Ma and X. Lei: Europhys. Lett. **67** (3) (2004) 432.
- 44) G. H. Ding, C. K. Kim and K. Nahm: cond-mat/0412502.
- 45) G. A. Lara, P. A. Orellana, J. M. Yáñez, E. V. Anda: Solid State Communications **136** (2005) 323.
- 46) P. W. Anderson, Phys. Rev. **124** (1961) 41.
- 47) P. A. M. Dirac: Canad. J. Math. **2** (1950) 129.
- 48) P. A. M. Dirac: *Lectures on Quantum Field Theory* (Belfer Graduate School of Science, Yeshiva University, New York, 1966).
- 49) P. A. M. Dirac: *Lectures on Quantum Mechanics* (Belfer Graduate School of Science, Yeshiva University, New York, 1964).
- 50) Strictly speaking, since the system is infinitely extended, local equilibrium states of the whole system can not be described by the density matrices.²² However, for the sake of simpler presentations, we use such notations.
- 51) A. L. Fetter and J. D. Walecka: *Quantum Theory of Many-Particle Systems* (Dover Publications, INC., Mineola, New York, 2003).
- 52) In contrast to the usual scattering problem, the perturbed Hamiltonian H_F does not have bound states, but the unperturbed one H_0 does.
- 53) R. G. Newton, *Scattering Theory of Waves and Particles* (Dover, New York, 2002); M. Kaku, *Quantum Field Theory* (Oxford University Press, Oxford, 1993).
- 54) B. Kubala and J. Köning: Phys. Rev. B **65** (2002) 245301.
- 55) A. Ueda, I. Baba, K. Suzuki and M. Eto: *Proc. Int. Conf. Quantum Transport and Quantum Coherence, Tokyo, 2002*, J. Phys. Soc. Jpn. **72**, (2003) Suppl. A, p.157-158.
- 56) M. Sato, H. Aikawa, K. Kobayashi, S. Katsumoto and Y. Iye: cond-mat/0410062.
- 57) A. Yacoby, M. Heiblum, D. Mahalu and H. Shtrikman: Phys. Rev. Lett. **15** (1995) 4047.
- 58) R. Schuster, E. Buks, M. Heiblum, D. Mahalu, V. Umansky and H. Shtrikman: Nature **385** (1997) 417.
- 59) L. Craco and K. Kicheon: Phys. Rev. B **59** (1999) 12244.
- 60) At first glance, the result of ref.38 does not agree with the present one. However, this discrepancy is an artifact because of the difference of the unit of the bias voltage. The authors of ref.38 measure the voltage in the unit of the Kondo temperature which increases faster than the peak width as n decreases. In the same unit, the two results agree well.
- 61) T.A. Costi and A.C. Hewson, Phil. Mag. B **65** (1992) 1165.
- 62) F. D. M. Haldane: Phys. Rev. Lett. **40** (1978) 416.

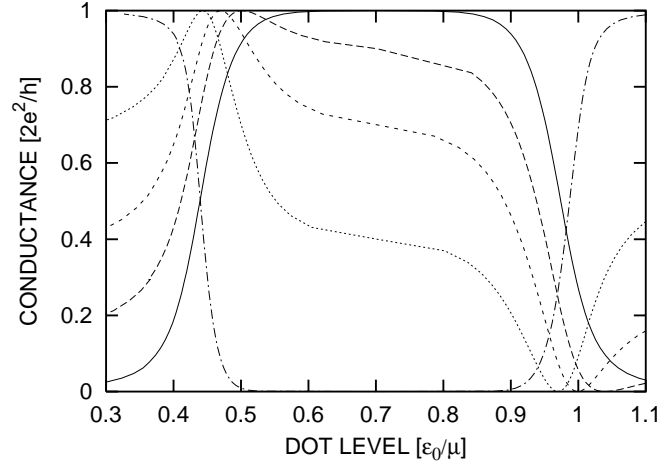


Fig. 1. The conductance in the linear-response regime as a function of the original dot level ϵ_0/μ , where $\varphi = 0$, $\Gamma/\mu = 0.02$ and the Coulomb interaction is $U/\mu = 0.6$ ($U/\Gamma = 30$) with μ the Fermi energy. Solid curve is the background transmission probability $T_b = 0.0$, the long-dashed curve at $T_b = 0.1$, the short-dashed curve at $T_b = 0.3$, the dotted curve at $T_b = 0.6$ and the dash-dotted curve at $T_b = 1.0$.

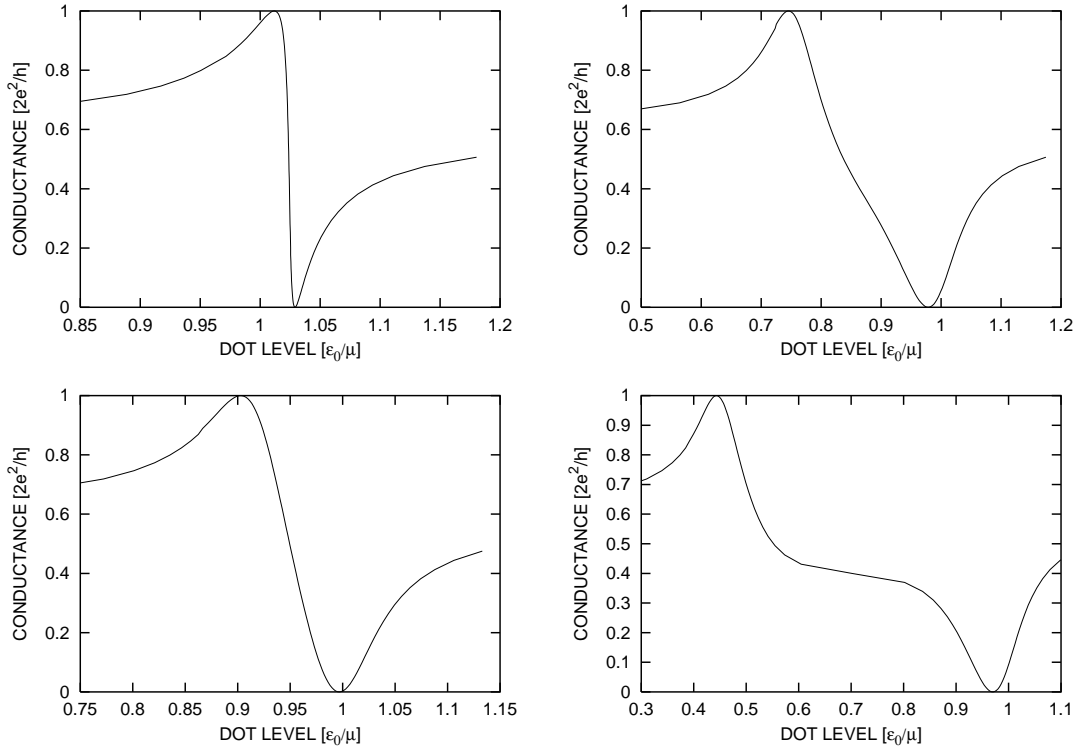


Fig. 2. The Coulomb interaction dependence of the conductance with $\varphi = 0.0$, $T_b = 0.6$. The Fano-Kondo plateau is formed with increasing the Coulomb interaction, the left side of the upper panel is for $U/\mu = 0.02$, the right side for $U/\mu = 0.3$ and the left side of the lower panel for $U/\mu = 0.14$, the right side for $U/\mu = 0.6$.

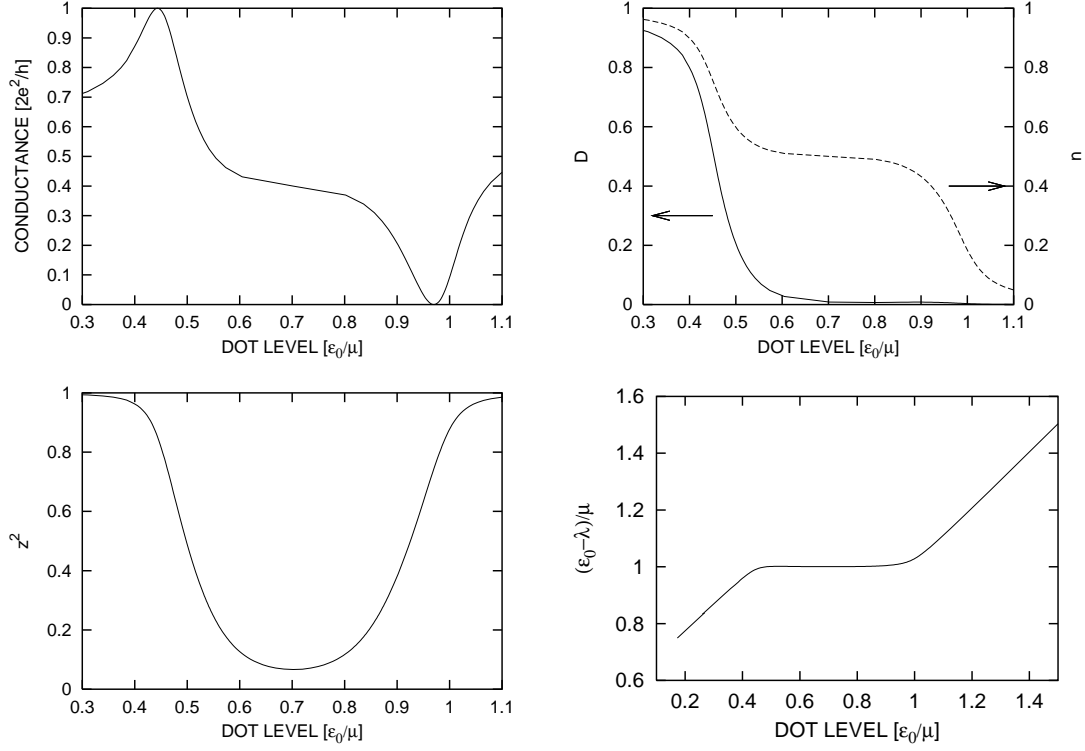


Fig. 3. SBMF parameters as functions of the dot energy. The left side of the upper panel is the differential conductance with $T_b = 0.6$, the right side is the electron occupation number and double occupation probability, the left side of the lower panel is the reduction factor of the dot level-width z^2 , and the right side is the renormalized dot energy as functions of the original dot level. The Coulomb interaction and AB phase are set to be $U/\Gamma = 0.6$, $\varphi = 0$.

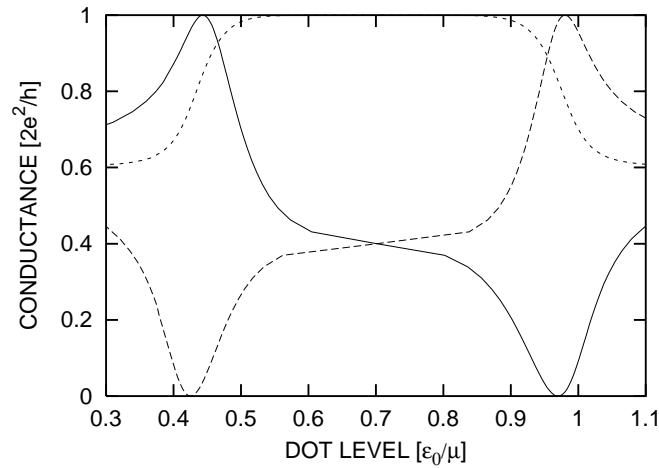


Fig. 4. The conductance for various values of the AB phase: $\varphi = 0$ (solid curve), $\varphi = \pi/2$ (short-dashed curve), $\varphi = \pi$ (long-dashed curve). The other parameters are set to be $T_b = 0.6$, $U/\mu = 0.6$.

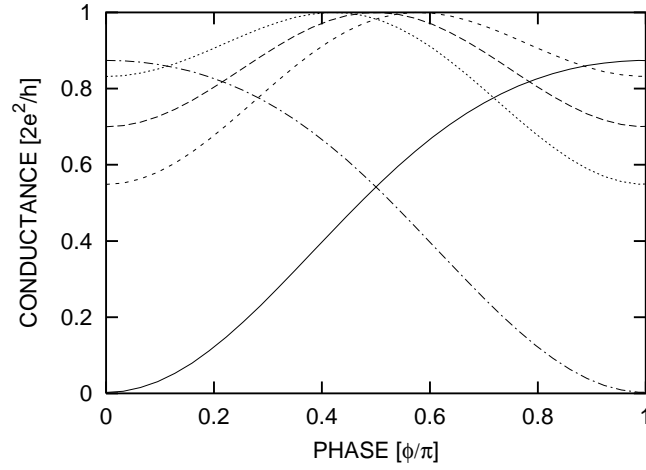


Fig. 5. AB oscillations as a function of the AB phase for the fixed electron occupation number with $T_b = 0.3$ and $U/\mu = 0.6$. Individual curves correspond to $n = 0.2$ (solid curve), $n = 0.45$ (short-dashed curve), $n = 0.5$ (long-dashed curve), $n = 0.55$ (dotted curve) and $n = 0.8$ (dash-dotted curve).

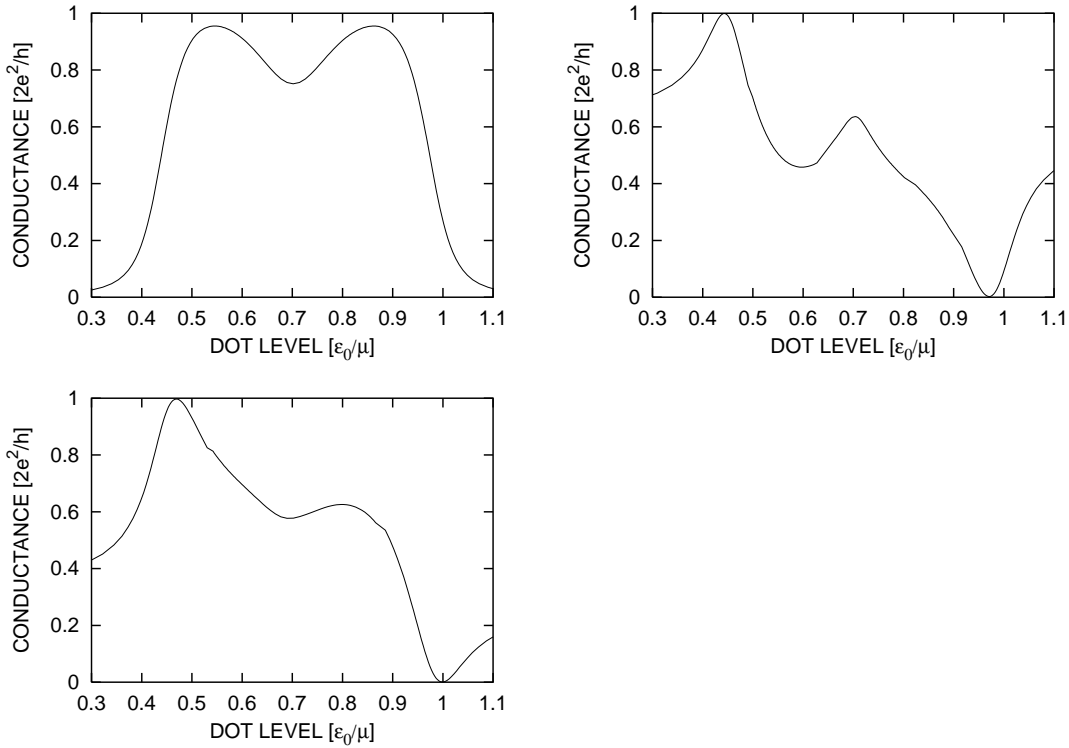


Fig. 6. Differential conductance at nonequilibrium regime as a function of the original dot level for several background transmission probabilities $T_b = 0.0$, $T_b = 0.6$ (left and right of upper panel) and $T_b = 0.3$ (left side of lower panel) with $\varphi = 0$, $U/\mu = 0.6$ and $eV/\mu = 0.002$.

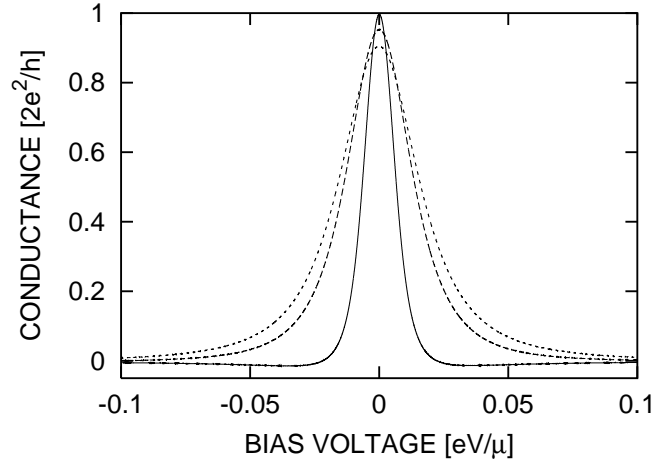


Fig. 7. The differential conductance as a function of the bias voltage with $T_b = 0.0$, $\varphi = 0$ and $U/\mu = 0.6$ for several fixed occupation numbers: $n = 0.48$ (solid curve), $n = 0.43$ (long-dashed curve) and $n = 0.40$ (short-dashed curve). At $n = 0.48$ and $eV/\mu = 0$, the conductance reaches the unitary limit.

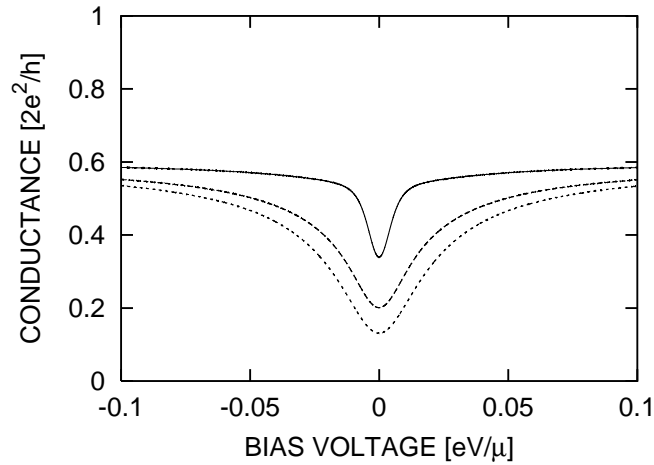


Fig. 8. The differential conductance as a function of the bias voltage with $T_b = 0.6$, $\varphi = 0$ and $U/\mu = 0.6$ for several fixed occupation numbers: $n = 0.48$ (solid curve), $n = 0.43$ (long-dashed curve) and $n = 0.40$ (short-dashed curve).

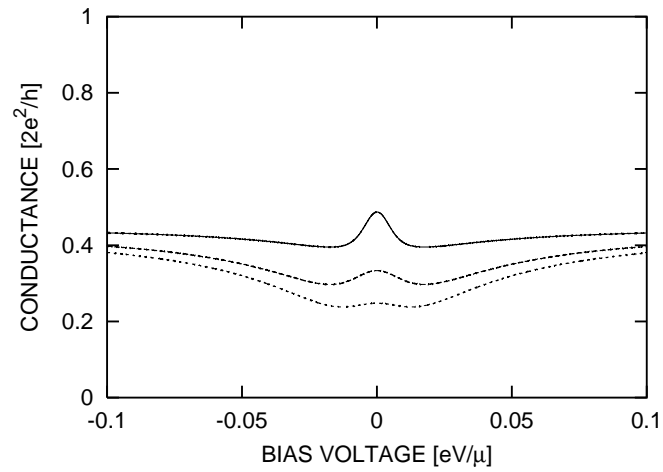


Fig. 9. The differential conductance as a function of the bias voltage with $T_b = 0.45$, $\varphi = 0$ and $U/\mu = 0.6$ for several fixed occupation numbers: $n = 0.48$ (solid curve), $n = 0.43$ (long-dashed curve) and $n = 0.40$ (short-dashed curve).